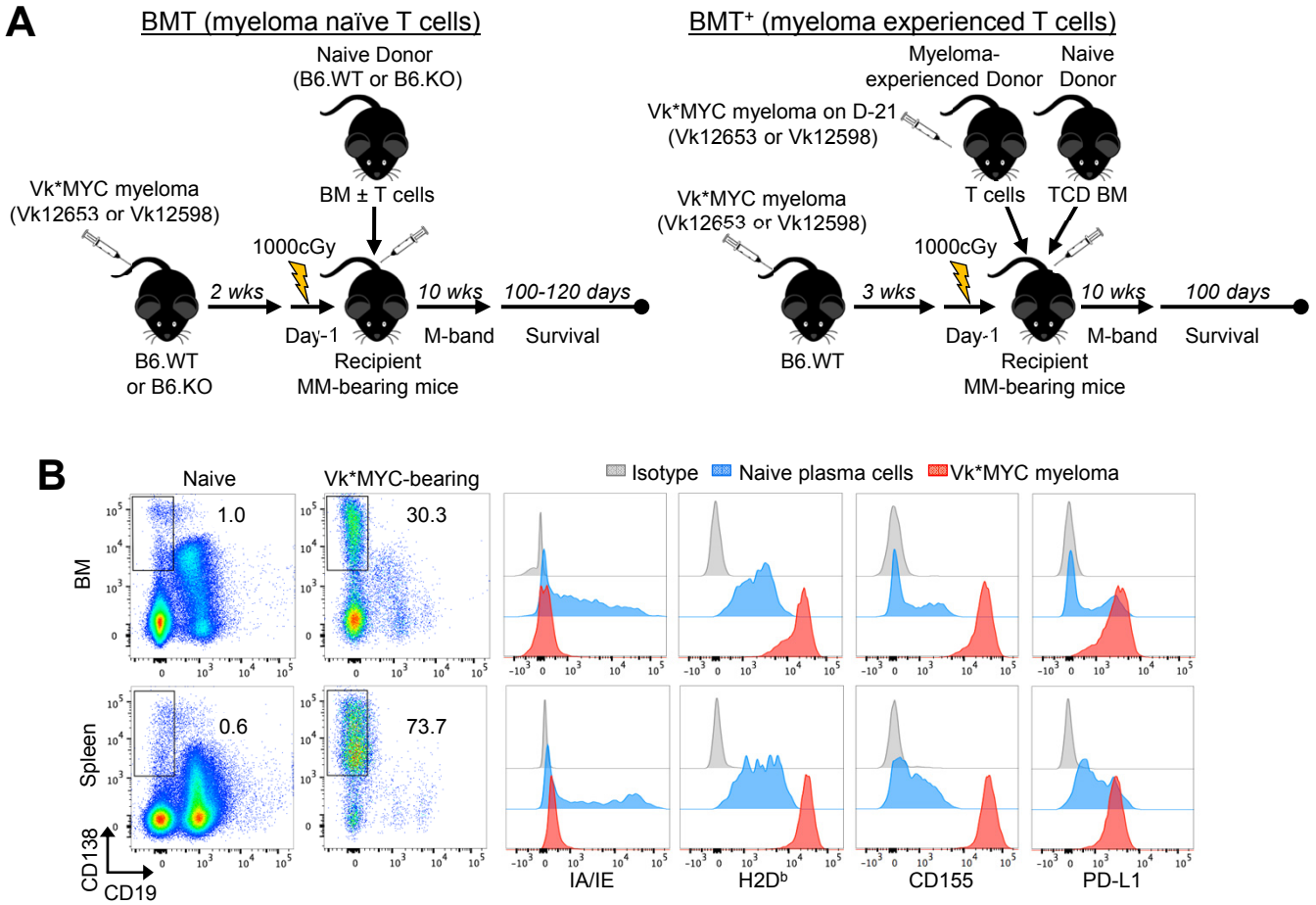

Supplementary Figure 1: Mouse models of BMT for myeloma.
(A) Illustration of transplantation models. **(B)** FACS plots of gating strategy for plasma cells ($CD19^{neg}CD138^{+}$) and histograms showing MHC Class II (IA/IE), MHC class I ($H2D^{b}$), CD155 and PD-L1 expression on plasma cells in naïve and Vk12653 bearing mice.

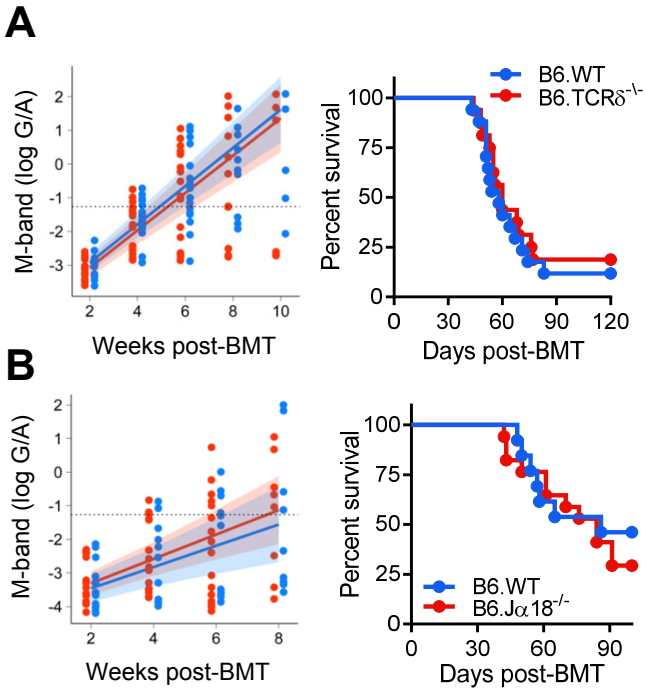

Supplementary Figure 2: Conventional T cells and not natural killer T cells control myeloma progression after BMT.
MM-bearing B6.WT mice were transplanted as previously described. Tumor burden and survival of Vk12653-bearing recipients transplanted with BM and T cells from **(A)** B6.WT or gamma delta T cell-deficient (TCR$\delta^{-/-}$) donors (*n* = 16 – 17 combined from 2 experiments), **(B)** B6.WT or natural killer T cell-deficient (Jα18$^{-/-}$) donors (*n* = 13 – 17 combined from 3 experiments).To determine statistical significance, tumor burden was plotted using longitudinal mixed effects linear models and survival was analyzed using a Log-rank test.

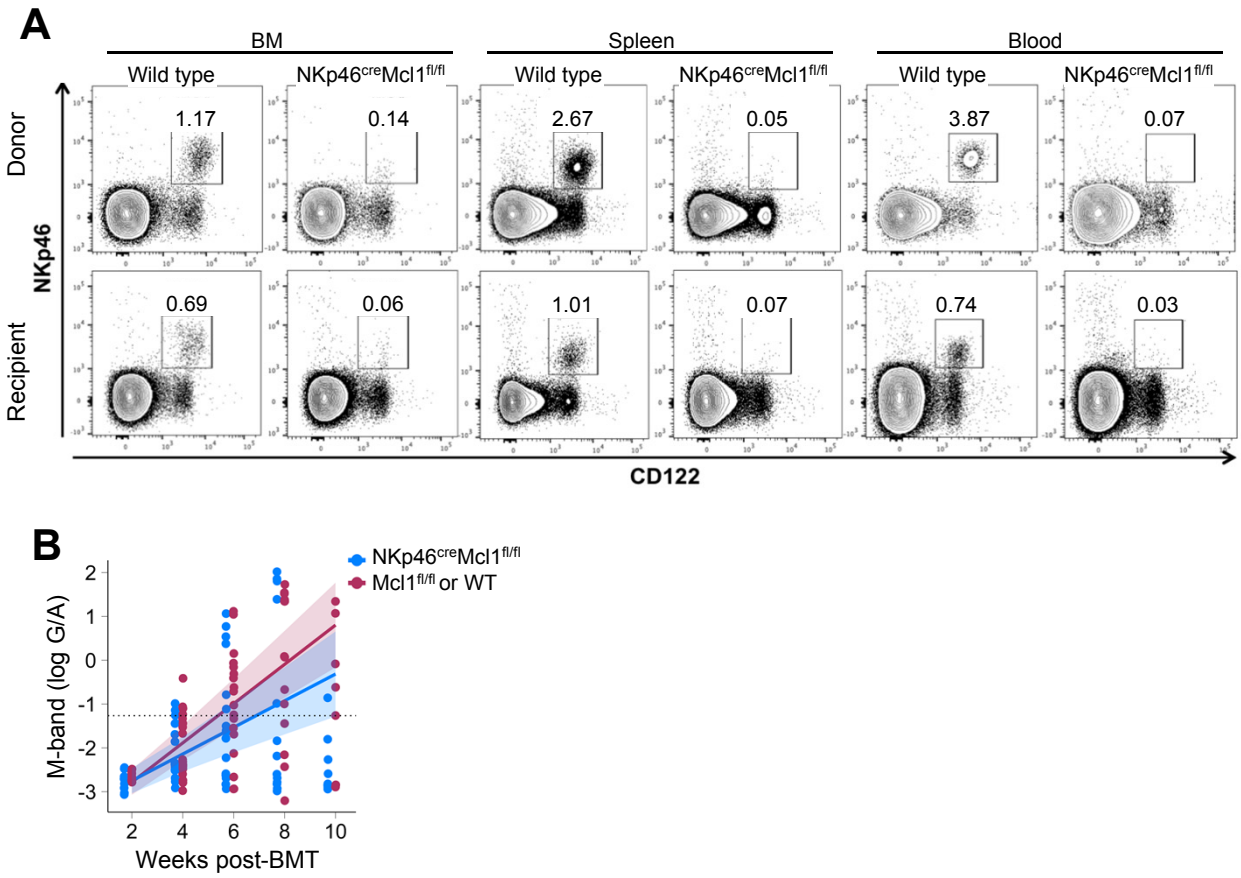

Supplementary Figure 3: Complete reconstitution of NK deficient donor grafts. MM-bearing B6 recipients were transplanted with B6.donor cells ($10x10^6$ BM and $5x10^6$ T cells) from NK intact ($Mcl1^{fl/fl}$ or wild-type (WT)) or NK cell-deficient ($NKp46^{cre}Mcl1^{fl/fl}$) donors **(A)** Representative FACS analyses show mature $NKp46^{+}CD122^{+}$ NK cells in BM, spleen and blood in donor grafts at time of transplant and in recipients at 120 days post-BMT. **(B)** M-band from transplanted recipients (n = 18 combined from 2 experiments).

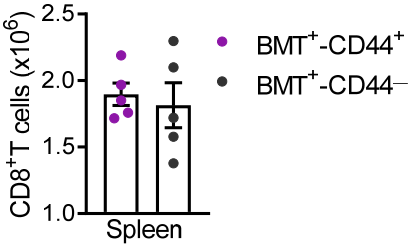

Supplementary Figure 4: CD8⁺ T cell number is unaffected in the spleen by memory composition of donor T cell graft after BMT⁺.
CD8+ T cell number in the spleen of MM-bearing recipients that were lethally irradiated and transplanted with 10 x 10^6 TCD-BM and 3 x 10^6 $CD44^+$ or $CD44^-$ T cells from CD45.1/CD45.2 myeloma-experienced donors.

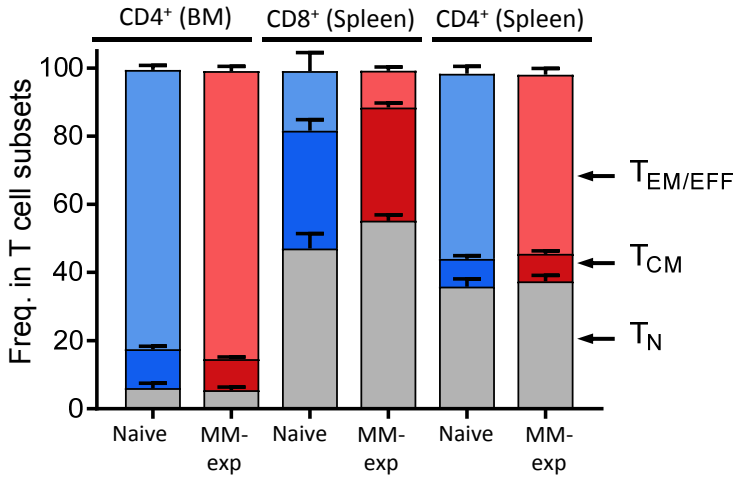

Supplementary Figure 5: T cell subsets in BM and spleen of recipients of naive or MM-experienced donor T cell grafts.

MM-bearing B6 recipients were transplanted with TCD-BM from naive B6 mice and either naive T cells (naive) or T cells from mice with long-term control of Vk12653 myeloma (>120 days post-BMT; MM-exp). Bars show distribution of $T_{EM/EFF}$, T_{CM} and T_N subsets (categorized by CD44 and CD62L expression) in $CD4^+$ T cells from the BM and $CD4^+$ and $CD8^+$ T cells from the spleen at 120 days post-BMT (n = 4 - 12 mice per group).

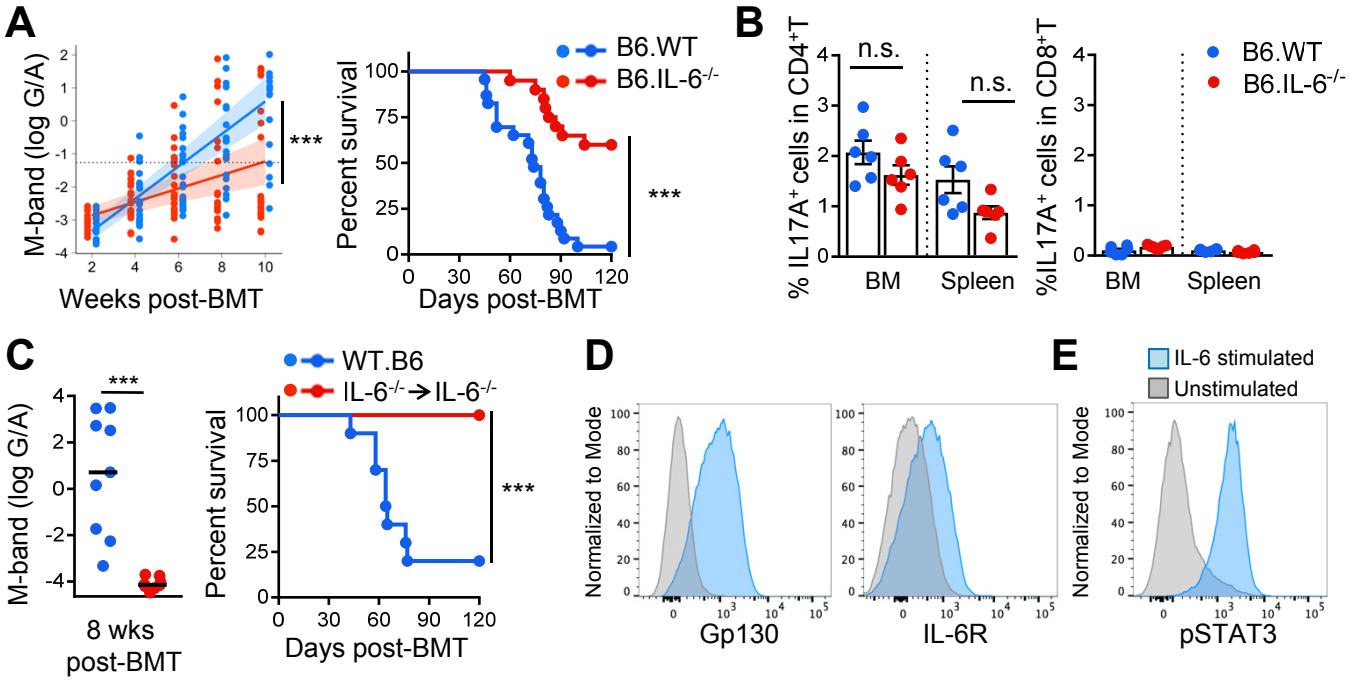

Supplementary Figure 6: IL-6 promotes myeloma relapse after BMT putatively by acting directly on the myeloma.

(A) Tumor burden, quantified using M-bands as described, and survival of MM-bearing recipients transplanted with BM ($10x10^6$) and T cells ($5x10^6$) from B6 wild-type (WT) or IL-6 deficient (IL-6$^{-/-}$) donors. Predictive rate of change of M-band indicated by solid line with confidence intervals shaded and M-band relapse threshold shown as dotted line (*n* = 20-23 from 3 experiments). **(B)** IL-17A production by CD4$^+$ T cells (Th17) and CD8$^+$ T cells (Tc17) in recipients of WT or IL-6 deficient grafts at 6 weeks post-BMT (n=6 from 1 experiment). **(C)** M-band at 8 weeks post-BMT and survival of MM-bearing IL-6 deficient recipients transplanted with IL-6 deficient grafts compared to WT recipients of WT grafts (*n* = 8-10 from 2 experiments). **(D)** Representative histograms showing Gp130 and IL-6R expression (blue; isotype in grey) and **(E)** constitutive and IL-6-induced (50ng/ml) phosphorylated STAT3 (pSTAT3) in Vk12653 myeloma cells (gated on CD19$^-$CD138$^+$) from BM (*n* = 3).***p<0.001.

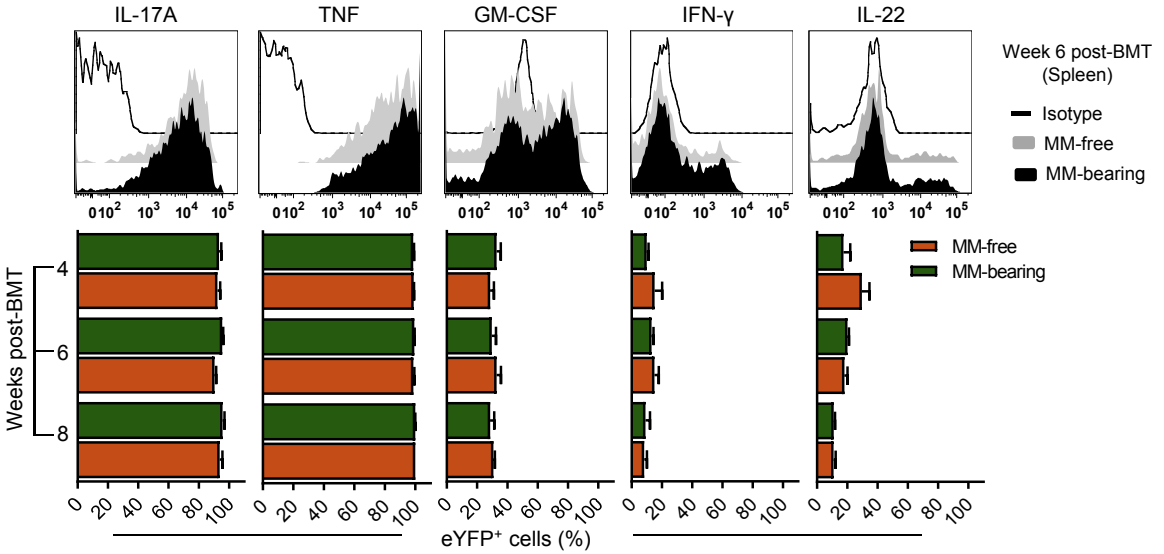

Supplementary Figure 7: Myeloma does not alter cytokine expression by T helper 17 cells after BMT.

MM-free and MM-bearing recipients were transplanted with BM and T cells from IL-17A^{Cre}Rosa26eYFP donors. eYFP^{+} cells were analyzed using flow cytometry in spleen and BM (femur). IL-17A, TNF, GM-CSF, IFNγ and IL-22 expression in eYFP^{+} cells at 4, 6 and 8 weeks post-transplant in the spleen of MM-free and MM-bearing recipients. Representative histograms are from spleen at week 6. (Week 4 and 8, *n* = *3* and week 6, *n* = 9 combined from 2 experiments).

Supplementary Table 1: TRBV gene usage in $CD8^+$ T cells from MM-free and MM-controlled mice.

	MM-free	MM-controlled	
TCR gene	**% Repertoire**		**Significance**
mTRBV1	0.75	0.67	N.S
mTRBV12-1	12.11	13.61	*p=0.0045*
mTRBV12-2	17.43	17.64	N.S
mTRBV13-1	9.35	8.91	N.S
mTRBV13-2	7.26	6.92	N.S
mTRBV13-3	9.01	9.39	N.S
mTRBV14	8.75	7.80	N.S
mTRBV15	1.80	1.65	N.S
mTRBV16	2.68	2.67	N.S
mTRBV17	3.48	3.25	N.S
mTRBV19	2.58	2.49	N.S
mTRBV2	2.23	2.46	N.S
mTRBV20	1.62	1.93	N.S
mTRBV23	0.04	0.06	*p=0.0007*
mTRBV24	0.03	0.03	N.S
mTRBV26	0.52	0.51	N.S
mTRBV29	6.07	5.37	*p=0.0443*
mTRBV3	5.74	5.78	N.S
mTRBV30	0.10	0.14	*p=0.0475*
mTRBV31	2.96	3.21	N.S
mTRBV4	2.12	2.10	N.S
mTRBV5	3.38	3.41	N.S

N.S = not significant

Supplementary Methods:

RNA-Seq RNA sequencing

To measure effects of IL-17A on myeloma, splenic myeloma cells (Vk12653) were sorted (purity >95%) and transplanted into RAGγc$^{-/-}$ mice. Mouse rIL-17A (BioLegend) or saline were administrated daily (1 μg/ip) for 7 days. Myeloma cells from the spleens of IL-17A or saline treated mice were sort-purified and processed for RNA sequencing by Macrogen (Seoul, South Korea). Sequence reads in each fastq file were trimmed for adapter sequences using Cutadapt (1) (version 1.11) and aligned using STAR (2) (version 2.5.2a) to the mm19 assembly with the gene, transcript, and exon features of Ensembl (release 75) gene model. Expression was estimated using RSEM (3) (version 1.2.30) and was used as input to assess differential gene expression between groups using the edgeR R package (4). Gene set enrichment analysis was performed using a 381 gene dataset of differentially expressed genes with uncorrected p-values of $p<0.05$ (5, 6).

TCR sequencing

MM-bearing (bearing Vk12653 myeloma) or MM-free recipients were transplanted with BM (CD45.1/2) and T cells (CD45.2). CD8^{+} T cells (CD45.2) were purified from spleen of MM-controlled (below relapse threshold) mice at day 56 post-BMT. TCR sequencing was performed by iRepertoire (Huntsville, AL) using custom built analysis pathways. Annotated repertoire files were downloaded from the iRepertoire website (http://www.irepertoire.com). Repertoires were first normalized by sampling an equal number of reads corresponding to the minimum number of reads sequenced across all samples to ensure the total abundance of all TCRs in each sample was equal. Percentage clonality was determined for each repertoire as the total abundance of the most enriched TCRs at each clonotypic number shared by the

abundance of all TCRs in the repertoire. Distribution of TCRs was determined by assigning each TCR an abundance level before the sum of each abundance level was calculated as a percentage of the entire repertoire. Shannon entropy and evenness scores for each repertoire were quantified as $-\Sigma p_i \ln p_i$ and $-\Sigma p_i \ln p_i / \ln S$, respectively, where p_i = proportion of S made up of the i^{th} species and S = total number of clonotypes in the repertoire. For entropy and evenness scores, the reads from all abundance clonotypes were resampled so that the total number of reads was again equal across all samples. The number of unique CDR3 sequences identified was determined by sampling each repertoire 10 times using the nominated read number before averaging the number of CDR3's detected across all replicates. TRBV and TRBJ gene usage was calculated as the proportional abundance of all TCRs of each gene relative to the abundance of all TCRs. T cell repertoire overlap was calculated based on the percentage of the repertoire that is residue-identical TCR (at the amino acid level) across donor pairs in each cohort.

Whole exome sequencing of Vk*MYC cells

Germline DNA is not available from the mouse in which the vk12653 line was established. Normal B cells isolated from C57BL/6 spleen were therefore used as germline control, accepting the caveat that genetic drift may account for a proportion of the tumour specific variants called (7) that may result in an overestimation of the mutational burden. DNA was extracted from FACS sorted Vk12653 cells, from the same in vivo passage used for experiments, and normal B cells isolated from C57BL/6 spleen. Whole exome sequencing was performed on Illumina Hiseq 4000 instruments by Macrogen (Seoul, South Korea). Library construction was performed using the SureSelectXT Library Prep Kit (Illumina) as per Illumina instructions and the subsequent 101 bp pair-end libraries were sequenced using TruSeq 3000 4000 SBS Kit v3. Resultant FASTQ files were used for analysis through the

following bioinformatics pipeline: a) alignment to the GRCm38(mm10) reference genome was performed using the Burrows-Wheeler Aligner (8) b) variant calling was performed using Samtools/BCFtools (9) c) functional annotation of the variants was achieved using ANNOVAR (10), including identification of SNPs present in dbSNP142. Following annotation, data was further filtered, requiring the following criteria to be met: a) the variant was not present in the sorted B cells isolated from C57BL/6 spleen; b) the variant was not present in the Sanger Centre Mouse Genome (https://www.sanger.ac.uk/science/data/mouse-genomes-project) sequencing of the C57BL/6 mouse strain; c) the vk12653 variant quality was >70; d) the vk12653 alternative read count was >2; e) an alternative read count being > 20% of the total read count. Furthermore, manual intervention was required for interpretation of variant calls in homologous gene families and from heavily duplicated regions.

References

1. Martin M. Cutadapt removes adapter sequences from high-throughput sequencing reads. *EMBnetjournal.* 2011;17(1):10-2.
2. Dobin A, Davis CA, Schlesinger F, Drenkow J, Zaleski C, Jha S, Batut P, Chaisson M, and Gingeras TR. STAR: ultrafast universal RNA-seq aligner. *Bioinformatics (Oxford, England).* 2013;29(1):15-21.
3. Li B, and Dewey CN. RSEM: accurate transcript quantification from RNA-Seq data with or without a reference genome. *BMC bioinformatics.* 2011;12(323.
4. Robinson MD, McCarthy DJ, and Smyth GK. edgeR: a Bioconductor package for differential expression analysis of digital gene expression data. *Bioinformatics (Oxford, England).* 2010;26(1):139-40.

5. Mootha VK, Lindgren CM, Eriksson KF, Subramanian A, Sihag S, Lehar J, Puigserver P, Carlsson E, Ridderstrale M, Laurila E, et al. PGC-1alpha-responsive genes involved in oxidative phosphorylation are coordinately downregulated in human diabetes. *Nature genetics.* 2003;34(3):267-73.

6. Subramanian A, Tamayo P, Mootha VK, Mukherjee S, Ebert BL, Gillette MA, Paulovich A, Pomeroy SL, Golub TR, Lander ES, et al. Gene set enrichment analysis: A knowledge-based approach for interpreting genome-wide expression profiles. *Proceedings of the National Academy of Sciences.* 2005;102(43):15545-50.

7. Casellas J. Inbred mouse strains and genetic stability: a review. *Animal : an international journal of animal bioscience.* 2011;5(1):1-7.

8. Li H, and Durbin R. Fast and accurate short read alignment with Burrows-Wheeler transform. *Bioinformatics (Oxford, England).* 2009;25(14):1754-60.

9. Li H, Handsaker B, Wysoker A, Fennell T, Ruan J, Homer N, Marth G, Abecasis G, and Durbin R. The Sequence Alignment/Map format and SAMtools. *Bioinformatics (Oxford, England).* 2009;25(16):2078-9.

10. Wang K, Li M, and Hakonarson H. ANNOVAR: functional annotation of genetic variants from high-throughput sequencing data. *Nucleic acids research.* 2010;38(16):e164.